Research Square

Preprints are preliminary reports that have not undergone peer review.
They should not be considered conclusive, used to inform clinical practice,
or referenced by the media as validated information.

CSCR insights in the Era of OCT-Angiography, sub-retinal fluid characteristics, choroidal flow abnormalities, and CSCR-related Choroidal Neovascular Membrane

Zeiad Eldaly

dr_ziadeldaly@aun.edu.eg

Assiut University Hospital

Hazem Abdelmotaal

Assiut University Hospital

Mahmoud Abdel-Radi

Assiut University Hospital

Marwa Abdellah

Sohag University Hospital

Mohamed Atito Hamed

Luxor University Hospital

Article

Keywords: Central serous chorioretinopathy, Choroidal hypoperfusion, Choroidal neovascular membrane, Optical Coherence Tomography Angiography

Posted Date: October 29th, 2026

DOI: https://doi.org/10.21203/rs.3.rs-10781315/v1

License: This work is licensed under a Creative Commons Attribution 4.0 International License.
Read Full License

Additional Declarations: No competing interests reported.

Abstract

Purpose

To evaluate morphological characteristics of sub-retinal fluid, RPE changes and choroidal blood flow in different sub-types of central serous chorioretinopathy using OCT-Angiography.

Methods

A cross-sectional observational study included consecutive series of 146 eyes with various sub-types of CSCR. OCT-A evaluated the characters of sub-retinal fluid and choroidal flow. Outcome measures included characters of high reflective foci in SRF, RPE abnormalities, CNV characters and distribution of vascular changes in choroidal vasculature.

Results

High reflective foci were found in 85% of eyes with persistent CSCR and in 22% eyes with chronic CSCR and none in acute CSCR. Fine dispersed high reflective foci were prevalent if SRF persistent less than 6 months while coarse clumped foci were obvious in fluid persistent more than 6 months. All eyes with acute and persistent CSCR exhibited abnormal choriocapillaris with patchy areas of hypoperfusion confined to area of SRF. Chronic CSCR displayed multifocal patchy areas of choriocapillaris hypoperfusion not bounded by areas of SRF. Choroidal slabs revealed dilatation of choroidal vessels as compared to fellow unaffected eyes. Flat irregular PED was found in 58.3% and neovascular frond was found in 30.1%. CNV area was variable (Mean; 0.289 mm^2) and variable patterns were detected. Larger CNV area significantly correlated with larger area of sub-retinal fluid.

Conclusion

OCT-A highlighted a difference in SRF characters and distribution of choroidal vascular changes among various CSCR subtypes along with identification of CSCR-related CNV.

Introduction

Central serous chorioretinopathy (CSCR) is a spectrum of clinical disorders that are characterized by serous macular detachment, retinal pigment epithelium (RPE) changes, and morphological choroidal vascular abnormalities.[1] It is predominantly affecting middle-aged men and often associated with corticosteroid use and psychosocial stress.[2] Visual impairment is attributed to persistence of macular detachment, RPE changes and development of CSCR-related choroidal neovascularization (CNV). [3]

CSCR encompasses a clinical spectrum ranging from acute to persistent, recurrent, and chronic CSCR depending on duration of subretinal fluid (SRF) and RPE/choroidal changes. [4]Various pathophysiological theories were postulated as autonomic dysregulation [5] and abnormal norepinephrine levels [6] that eventually lead to choroidal hyperpermeability. Type A personality [7], obstructive sleep apnea [8], H. Pylori infection, [9] and exogenous corticosteroid [10] are common associations with CSCR.

Fundus Fluorescein Angiography (FFA) [11], Indocyanine Green (ICG) [12], Fundus Auto-Fluorescence (FAF), [13] and Optical Coherence Tomography (OCT) [14 15] were employed for diagnosis and follow up of CSCR in different stages. OCT angiography is a high-resolution non-invasive imaging of microvascular changes in retinal and choroidal layers. OCTA permits the detection of CNV associated with flat irregular PED in CSCR, an area often underdiagnosed by conventional imaging[16 17 18].

We intended to analyze the spectrum of morphological changes of sub-retinal fluid, RPE, and choroidal blood flow in different sub-types of CSCR using OCT-A and to assess their correlation with disease duration.

Patients and methods

Study design

A cross-sectional observational study was conducted after approval of the Ethical Committee of the Faculty of Medicine, Assiut University, Egypt. A signed informed consent was obtained from participants after discussion of the procedure and its possible benefits and risks. All study procedures were performed under the tenets of the Helsinki Declaration.

Patient selection

The study enrolled a consecutive series of 82 patients, attending retina clinic, diagnosed with CSCR based on multimodal imaging and clinical history. CSCR were categorized into acute, persistent and chronic subtypes. [19] Acute CSCR usually presented with isolated dome-shaped neuro-sensory retinal elevation without RPE changes that persist less than 4 months, while persistent CSCR had SRF that persisted beyond 4 months with no significant RPE changes. In chronic CSCR, the chronic leakage of SRF tends to produce a larger, less elevated neuro-retinal detachment along with significant RPE changes. Exclusion criteria were; evidence of concurrent retinal vascular disease (e.g., diabetic retinopathy), presence of high myopia or other macular pathology (choroidal neovascular membrane, macular edema), history of intraocular surgery or injections within the previous 6 months, and poor-quality OCT or OCTA images due to media opacity or unstable fixation.

Baseline evaluation

Baseline clinical evaluation was carried out by a single ophthalmologist (Z. E.) and included patient demographic data, past ocular and medical history, onset of symptoms (metamorphopsia, micropsia,

decreased vision), best-corrected visual acuity (BCVA), Slit-lamp examination, IOP measurement by Goldmann Applanation Tonometer and fundus examination using + 90 D non-contact fundus lens.

OCT-Angiography protocol

All participants underwent OCT and OCT-A imaging using the Topcon Triton DRI OCT-A platform (Topcon, Tokyo, Japan) with a 6 mm X 6 mm scan area centered around fovea. In addition, 3D-macular analysis was also acquired for Enface OCT-A assessment. Two independent investigators (Z. E. and M. A.) evaluated OCT and OCT-A images for CSCR phenotype analysis, image quality, and artifact detection. Images with sufficient quality (signal strength index more than 50) were included, while images of poor quality due to severe motion artifact or media opacity were excluded. Subfoveal choroidal thickness was measured in subfoveal point between Sclero-choroidal interface (SCI) and outer boundary of RPE-Bruch's membrane complex. Sub-retinal fluid was analyzed by En-face OCT-A for the presence of high reflective foci (HRF) and their distribution was correlated with sub-type of CSCR. HRF were defined as hyperreflective dots within the SRF space and were further classified as fine/dispersed or coarse/clumped, based on reflectivity patterns and size. Choriocapillaris and deep choroidal vessels were evaluated across the choroidal slabs (Haller’s and Sattler’s layers). We assessed vessel dilation, choriocapillaris (CC) perfusion deficits, and shadowing artifacts caused by SRF. CC perfusion deficits were identified as black areas of hypoperfusion within CC, on the other hand SRF shadowing outline was identified as areas of reduced signal compared to adjacent areas of average signal. Areas with flat irregular pigment epithelial detachment (FI-PED) were assessed for the presence of CNV. Both quantitative and qualitative analysis of CNV characteristics were ensued. FI-PED was defined as RPE elevation with a non-convex profile, accompanied by irregular reflectivity. CNV fronds were characterized by their morphology—branching, immature, or poorly delineated—and quantified using automated segmentation tools. The CNV area was measured in mm^2, and flow signals were analyzed using proprietary algorithms.

OCT-A slabs were manually adjusted to ensure proper segmentation and reduction of artifacts (especially projection artifacts). In Enface OCT-A analysis of SRF, manual adjustment of slabs was performed with device software. First, flattening of RPE was performed using device software option, then slabs were adjusted along flattened RPE (outer boundary) and along the highest point within the SRF that include HRF (inner boundary). Analysis of choriocapillaris image was obtained by slabs between 30 and 60 μm below the RPE-Bruch's membrane complex. OCT-A slabs for assessment of choroidal vessels were manually adjusted just above outer boundary of visible SCI and just below choriocapillaris.

Statistical Analysis

Descriptive statistics were presented as means ± standard deviations for continuous variables and frequencies (%) for categorical data. Comparative analysis across CSCR subtypes employed the chi-square test for categorical variables and ANOVA for continuous measures. Correlation between CNV

area and SRF area was assessed using Pearson's correlation coefficient. A p-value < 0.05 was considered statistically significant. Data were analyzed using SPSS software (V 25.0, IBM, USA).

Results

A total of 82 patients (157 eyes) diagnosed with CSCR were enrolled in the study. Eleven eyes were excluded from analysis due to poor image quality or significant artifact. Remaining 146 eyes were subjected to CSCR stratification, OCT, and OCT- A assessment. The mean age of participants was 50.9 ± 9.3 years (range; 29-62 years). Subjects were stratified into acute (38 eyes), persistent (58 eyes), or chronic CSCR (50 eyes) based on medical history, clinical presentation, and retinal imaging. Such classification provided a framework for comparative analysis of morphological and angiographic characteristics across the disease spectrum.

Subfoveal choroidal thickness

Analysis of subfoveal choroidal thickness (SFCT) revealed a declining trend from acute to chronic subtypes. Acute CSCR demonstrated the highest mean SFCT at 538 µm, followed by persistent CSCR with 528 µm. Chronic CSCR had the lowest choroidal thickness (437 µm). (Table 1)

En face OCT-A of subretinal fluid

En face OCT-A imaging revealed a remarkable diversity in the morphology of HRF in different CSCR subtypes. HRF were not identified in any eyes with acute CSCR. In contrast, most of eyes diagnosed with persistent CSCR exhibited HRF, regardless of fluid duration. HRF were detected in only 11 of 50 chronic CSCR eyes (22 %). The morphology of HRF varied according to the duration of SRF; persistent SRF for less than 6 months had fine, dispersed HRF, while those with SRF more than 6 months demonstrated coarse, clumped foci. This difference in HRF morphology across duration thresholds was significant (chi-square test, p = 0.013), underscoring HRF as a potential imaging biomarker for persistent disease. (Figure 1)

OCT-A evaluation of choriocapillaris perfusion

Evaluation of CC perfusion demonstrated distinctive patterns across disease subtypes. In acute and persistent CSCR, areas of CC hypoperfusion were typically localized beneath SRF and often accompanied by shadowing artifacts due to fluid accumulation. Among those patients with acute and persistent CSCR, 68 of 96 eyes (70.8%) exhibited detectable shadowing effects, indicating partial signal attenuation due to overlying subretinal material. Deep choroidal slabs across Haller and Sattler's layers revealed obvious dilatation of choroidal vessels as compared to fellow unaffected eyes. In contrast, chronic CSCR was characterized by multifocal, patchy CC flow voids extending well beyond SRF-affected zones, suggesting a more diffuse and potentially irreversible vascular compromise not limited to active detachment areas or areas with persistent SRF. (Figure 2)

Assessment of Flat irregular pigment epithelial detachment (FI-PED)

FI-PED were identified in 63 of the 108 eyes (58.3%) with persistent and chronic CSCR. No FI-PED was detected in acute CSCR. Among these, CNV was detected in 33 eyes (30.1%) on OCT-A imaging. Most FI-PEDs displayed high internal reflectivity (26 of 37 eyes, 70.3%), a feature frequently associated with underlying neovascular networks. CNV area was quantitatively analyzed and revealed a mean size of 0.289 ± 0.394 mm², with a range spanning from 0.193 to 0.779 mm². A significant positive correlation was observed between the CNV area and the area of SRF (Pearson correlation coefficient $r = 0.428$, $p = 0.039$). (Table 2)

CNV morphology by OCT-A

Regarding CNV morphology, three distinct types were recognized: branching CNV (12 eyes, 36.4%), immature CNV (17 eyes, 51.5%), and poorly delineated CNV (4 eyes, 12.1%). Branching vascular networks were predominantly observed in cases with wider FI-PED, while immature or poorly-defined CNV patterns were more commonly noted in earlier stages of neovascular development. (Figure 3)

Discussion

The current study investigated the potential advantage of OCT and OCT angiography in characterizing CSCR, with a particular emphasis on their roles in differentiating disease subtypes and detecting non-leaking CNV. Current results demonstrate that OCT and OCT-A together offer a comprehensive, non-invasive diagnostic approach that not only enhances the visualization of morphological markers such as HRF and FI-PED but also allows the detection of subclinical neovascular membranes that might otherwise remain undiagnosed using conventional imaging modalities as FFA.

Reduction in choroidal thickness with chronicity of CSCR supports the concept of long-term choroidal remodeling and vascular decompensation in chronic CSCR. On the other hand, patchy CC flow voids in chronic CSCR extended well beyond the boundaries of SRF, suggesting that a prolonged period of pachychoroidopathy might eventually affect the choroid globally rather than areas with overlying subretinal fluid.

One of the most significant findings of our study was the variable distribution and morphology of HRF across CSCR subtypes. HRF were absent in all acute cases, in most of cases of persistent CSCR, and detected in only a small fraction of chronic CSCR eyes. This finding aligns with prior work by Spaide and colleagues, who proposed that HRF may represent cellular debris, outer segment fragments, activated microglia, or migrating RPE cells accumulating over time as a response to chronic subretinal fluid. [20] Our data further substantiate the hypothesis that HRF serve as a dynamic biomarkers of disease chronicity. Interestingly, we observed a qualitative shift in HRF morphology based on SRF duration—fine and dispersed HRF appeared in cases with fluid lasting less than six months, while coarse and clumped HRF emerged in eyes with more prolonged exudation.

Current findings are in concordance with prior literature, including the work by Ho et al, who identified coarse, granulated hyperreflective signals in persistent CSCR on OCT-A, correlating these with ischemia and inflammatory cell accumulation. [21]This morphologic stratification may hold prognostic implications, suggesting a transition point where persistent fluid initiates irreversible retinal changes. While, HRF were present in only 22% of cases with chronic CSCR, suggesting a potential biphasic behavior where HRF density peaks during intermediate disease and may regress or become less apparent as outer retinal atrophy progresses. [22] [23] (Table 3)

CC perfusion analysis provided additional insight into the vascular changes in CSCR. In acute and persistent subtypes, hypoperfusion of the CC was generally confined to areas underlying SRF and was frequently associated with signal attenuation or shadowing. Taking into consideration that shadowing of overlying SRF may contribute in signal attenuation of CC especially with high SRF. In chronic cases, however, OCT-A revealed widespread, multifocal flow voids extending beyond the SRF footprint. These findings reflected those reported by Pellegrini et al. [26] and Imamura et al. [24], who described that progressive choroidal hypoperfusion in chronic CSCR could be attributed to chronic RPE dysfunction and pachychoroid vasculopathy. Importantly, the current observation that CC loss occurs even in regions without visible fluid suggests a deeper, perhaps microvascular dysregulation characteristic of pachychoroid-spectrum disorders. This hypothesis is supported by previous studies, including those by Matet et al. [25] and Kaye et al. [26], both of which described progressive CC ischemia in chronic CSCR. Current findings are in agreement with longitudinal data published by Bansal et al. [27] and Pellegrini et al. [28], both of whom reported sustained CC signal changes and evolving neovascular features in chronic CSCR over time.

The presence of FI-PED among CSCR patients was not uncommon and CSCR-related CNV was detected in half of those cases. Most of these CNV lesions were not evident on structural OCT or FFA, underscoring the superior sensitivity of OCT-A in identifying neovascularization that is either non-exudative or minimally active. Moreover, about two-thirds of neovascular fronds detected by OCT angiography were either immature CNV (51.5%) or poorly delineated CNV (12.1%). CNV features in OCT angiography needed meticulous adjustment of OCT slabs and careful interpretations. The significant correlation between CNV and SRF area ($p = 0.039$) may indicate a potential link between persistent fluid and neovascular proliferation. These findings are consistent with various studies by Mousa et al., Costanzo et al., and Huang et al., that reported CNV detection rates of 30–60% in chronic CSCR using OCT-A. [18] [29] [30] Notably, we also found a statistically significant correlation between CNV area and SRF area, suggesting a potential pathophysiological interplay in which persistent exudation may stimulate angiogenesis through chronic RPE stress and hypoxia.

OCT-A diagnostic performance in the current study supports its growing participation as a critical tool for retino-choroidal vascular assessment. Numerous large-scale studies, including those by Bonini Filho et al. [31] and Hagag et al. [32], have confirmed that OCT-A offers higher sensitivity and specificity than FA or ICGA for detecting CNV, particularly in non-leaking forms. The current findings reinforce this advantage

within the context of CSCR, where FI-PED and ambiguous fluid patterns often obscure the clinician's ability to distinguish inflammatory or degenerative changes from neovascular pathology. OCT-A overcomes this challenge by providing high-resolution, depth-resolved visualization of vascular flow, even in the absence of leakage. Our findings further substantiate the premise that OCT-A reveals neovascular changes that are often missed by FA or structural OCT. This is particularly critical in non-leaking or type 1 CNV, where absence of leakage on dye angiography may delay diagnosis and treatment. The identification of CNV at a pre-exudative stage enables earlier initiation of anti-VEGF therapy or photodynamic therapy (PDT), potentially preserving vision and preventing chronic damage. (Table 4)

While current cross-sectional design enabled detailed comparative analysis across disease stages, it precludes assessment of longitudinal progression. Future prospective studies could determine whether HRF density, CC perfusion deficits, or CNV area on OCT-A predict anatomical or visual outcomes over time. Additionally, although swept-source OCT-A minimized artifacts, segmentation errors and shadowing from SRF remain potential confounders in quantitative vascular analysis. However, the consistency of findings across subgroups and the strong concordance with prior literature mitigate this concern.

Conclusion

The findings of the current study confirm the clinical utility of OCT and OCT-A in delineating structural and vascular changes across CSCR subtypes. The OCT & OCT-A findings regarding HRF, CC perfusion, and CNV highlight the importance of incorporating OCT-A in routine CSCR evaluation for early identification of disease progression and complications. The presence of high reflective foci and their density is associated with a longer duration of sub-retinal fluid in persistent CSCR. In most cases, choriocapillaris hypoperfusion was observed with diverse distribution among different CSCR sub-types. Choroidal vessels revealed obvious dilatation. Most of CNV related to FI-PED had an immature neovascular frond. We propose that OCT-A should be adopted as a routine adjunct to structural OCT in all patients with persistent or chronic CSCR, especially in cases with flat irregular PEDs or unexplained visual decline. Early detection of CNV and characterization of perfusion deficits may not only clarify diagnosis but also guide timely therapeutic interventions, potentially preserving vision and altering disease trajectory.

Declarations

Acknowledgment

No acknowledgment to be declared

Funding

No funding was received for this research.

Conflict of Interest

All authors certify that they have no affiliations with or involvement in any organization or entity with any financial interest or non-financial interest in the subject matter or materials discussed in this manuscript.

Data Availability

The datasets generated and/or analyzed during the current study are available from the corresponding author upon request.

Author Contributions statement

HA was responsible for writing the protocol and report, making research plan and reviewing literature, interpreting results. MAR was responsible for writing the protocol and reviewing literature and updating reference lists. MA was responsible for writing the protocol and report, making research plan and reviewing literature, interpreting results. MAH was responsible for making research plan and reviewing literature, and interpreting results. ZE was responsible for writing the manuscript, extracting, analyzing data, interpreting results and conducted the statistical analysis.

References

1. Liew G, Quin G, Gillies M, Fraser-Bell S. Central serous chorioretinopathy: a review of epidemiology and pathophysiology. Clin Exp Ophthalmol. 2013;41:201–14.
2. Zhang X, Lim CZF, Chhablani J, Wong YM. Central serous chorioretinopathy: updates in the pathogenesis, diagnosis and therapeutic strategies. Eye Vis (Lond). 2023;10(1):33.
3. Dansingani KK, Balaratnasingam C, Naysan J, Freund KB. En face imaging of pachychoroid spectrum disorders with swept-source optical coherence tomography. Retina. 2016;36:499-516.
4. Quaranta-El Maftouhi M, El Maftouhi A, Eandi CM. Chronic central serous chorioretinopathy imaged by optical coherence tomographic angiography. Am J Ophthalmol. 2015;160(3):581-587.e1.
5. Tewari HK, Gadia R, Kumar D, et al. Sympathetic-parasympathetic activity and reactivity in central serous chorioretinopathy: A case-control study. Invest Ophthalmol Vis Sci. 2006;47:3474-8.
6. Samanta A, Gregori G, Muzi A, et al. Optical Coherence Tomography Study of Choroidal Response to Exercise-Induced Hypertension in Chronic Central Serous Chorioretinopathy. J Clin Med. 2024;13(21):6580.
7. Wong KH, Lau KP, Chhablani J, Tao Y, Li Q, Wong IY. Central serous chorioretinopathy: what we have learnt so far. Acta Ophthalmol. 2016;94(4):321-325.
8. Yavaş GF, Küsbeci T, Kaşikci M, et al. Obstructive sleep apnea in patients with central serous chorioretinopathy. Curr Eye Res. 2014;39:88-92.
9. Cotticelli L, Borrelli M, D'Alessio AC, et al. Central serous chorioretinopathy and Helicobacter pylori. Eur J Ophthalmol. 2006;16(2):274-278.

10. Van Dijk EH, Nijhoff MF, de Jong EK, et al. Central serous chorioretinopathy in primary hyperaldosteronism. Graefes Arch Clin Exp Ophthalmol. 2016;254: 2033–42.
11. Shahin MM. Angiographic characteristics of central serous chorioretinopathy in an Egyptian population. Int J Ophthalmol. 2013;6(3):342-5.
12. Tsujikawa A, Ojima Y, Yamashiro K, et al. Punctate hyperfluorescent spots associated Detection of Silent Type I Choroidal Neovascular Membrane in Chronic Central Serous Chorioretinopathy Using En Face Swept-Source Optical Coherence Tomography Angiography with central serous chorioretinopathy as seen on indocyanine green angiography. Retina. 2010;30:801-9.
13. Spaide RF, Klancnik JM, Klancnik J Jr. Fundus autofluorescence and central serous chorioretinopathy. Ophthalmology. 2005;112:825-33.
14. Lehmann M, Wolff B, Vasseur V, et al. Retinal and choroidal changes observed with 'En face' enhanced-depth imaging OCT in central serous chorioretinopathy. Br J Ophthalmol. 2013;97(9):1181-6.
15. Hamzah F, Shinojima A, Mori R, Yuzawa M. Choroidal thickness measurement by enhanced depth imaging and swept-source optical coherence tomography in central serous chorioretinopathy. BMC Ophthalmol. 2014;25;14:145..
16. Costanzo E, Cohen SY, Miere A, et al. Optical coherence tomography angiography in central serous chorioretinopathy. J Ophthalmol. 2015;2015:134783.
17. Chan SY, Wang Q, Wei WB, Jonas JB. Optical coherence tomographic angiography in central serous chorioretinopathy. Retina. 2016;36:2051-8.
18. Moussa M, Leila M, Khalid H, Lolah M. Detection of Silent Type I Choroidal Neovascular Membrane in Chronic Central Serous Chorioretinopathy Using En Face Swept-Source Optical Coherence Tomography Angiography. J Ophthalmol. 2017;2017:6913980.
19. van Rijssen TJ, van Dijk EHC, Yzer S, et al. Central serous chorioretinopathy: Towards an evidence-based treatment guideline. Prog Retina Eye Res. 2019;73:100770.
20. Spaide RF. Choriocapillaris flow features following treatment of chronic central serous chorioretinopathy with photodynamic therapy. Retina. 2018;38(4):729–40.
21. Ho M, Li G, Mak A, et al. Applications of Multimodal Imaging in Central Serous Chorioretinopathy Evaluation. J Ophthalmol. 2021;2021:9929864.
22. de Carlo TE, Bonini Filho MA, Chin AT, et al. Spectral-domain OCT angiography of choroidal neovascularization. Ophthalmology. 2015;122(6):1228–38.
23. Bianchi M, Sarraf D, Freund KB. En face OCT findings of hyperreflective foci in central serous chorioretinopathy. Ophthalmic Surg Lasers Imaging Retina. 2019;50(10):e268–71.
24. Imamura Y, Fujiwara T, Margolis R, Spaide RF. Enhanced depth imaging optical coherence tomography of the choroid in central serous chorioretinopathy. Retina. 2009;29(10):1469–73.
25. Matet A, Daruich A, Dirani A, et al. Insights into pathology of chronic central serous chorioretinopathy: A cross-sectional study. Retina. 2019;39(5):889–99.

26. Kaye R, Chandra S, Sheth J, et al. Central serous chorioretinopathy: An update on risk factors, pathophysiology and imaging modalities. Prog Retina Eye Res. 2020;79:100865.
27. Bansal R, Dogra M, Mulkutkar S, et al. Optical coherence tomography angiography versus fluorescein angiography in diagnosing choroidal neovascularization in chronic central serous chorioretinopathy. Indian J Ophthalmol. 2019 Jul;67(7):1095-1100.
28. Pellegrini M, Fossataro F, Borrelli E, et al. OCT angiography findings in patients with central serous chorioretinopathy. Br J Ophthalmol. 2019;103(10):1370–5.
29. Huang YS, Lee CL, Yang CM. The role of optical coherence tomography angiography in detecting choroidal neovascularization in chronic central serous chorioretinopathy. Am J Ophthalmol. 2014;158(3):672–80.
30. Costanzo E, Cohen SY, Semoun O, et al. Optical coherence tomography angiography in central serous chorioretinopathy. J Ophthalmol. 2015;2015:134783.
31. Bonini Filho MA, de Carlo TE, Ferrara D, et al. Association of Choroidal Neovascularization and Central Serous Chorioretinopathy with Optical Coherence Tomography Angiography. JAMA Ophthalmol. 2015 Aug;133(8):899-906.
32. Hagag AM, Rasheed R, Chandra S, et al. The Diagnostic Accuracy of Double-Layer Sign in Detection of Macular Neovascularization Secondary to Central Serous Chorioretinopathy. Am J Ophthalmol. 2022 Apr;236:271-280.

Tables

Table 1: Baseline demographic and clinical characteristics

	Acute (n=38)	Persistent (n=58)	Chronic (n=50)
Age (years)	48.2 ± 7.1	52.1 ± 9.4	53.6 ± 8.9
Gender (M/F)	(20/18)	(37/21)	(22/28)
BCVA (Decimal)	0.6 ± 0.09	0.4 ± 0.12	0.3 ± 0.16
Duration of symptoms (months)	2.8 ± 1.3	9.3 ± 2.1	16.1 ± 5.2
Pattern of symptoms			
Decreased vision	15 (39.5%)	18 (31.1%)	47 (94.0%)
Metamorphopsia	25 (65.9%)	38 (65.5%)	13 (26.0%)
Micropsia	12 (31.6%)	9 (15.5%)	11 (22.0%)
Subfoveal choroidal thickness (µm)			
Subfoveal choroidal thickness (µm)	538	528	437
High reflective foci (HRF)			
HRF (n, %)	0	49/58 (84.5%)	11/50 (22%)
FI-PED			
Present (n, %)	0	19/58 (32.8%)	44/50 (88.0%)
CNV by OCT-A (n, %)	0	4/58 (6.9%)	29/50 (58.0%)

CNV; Choroidal neovascular membrane, FI-PED; Flat irregular PED, High reflective Foci; HRF

Table 2: CNV Characteristics in Eyes with Flat Irregular PED

CNV Parameter	
CNV detected by OCT-A (n, %)	33/108 (30.1%)
Mean CNV area (mm²)	0.289 ± 0.394
CNV area range (mm²)	0.193 – 0.779
Correlation with SRF area	r = 0.428, p = 0.039 Pearson correlation coefficient
CNV morphology	
Branching	12 eyes (36.4%)
Immature	17 eyes (51.5%)
Poorly defined	4 eyes (12.1%)

CNV; Choroidal neovascular membrane

Table 3: Evidence supporting HRF relation to SRF and disease duration

Study (Year)	Sample Size (Eyes)	Prevalence	Study Conclusion
Spaide RF (2018)	67	72% in persistent CSCR	HRF density increases with longer SRF duration; associated with inflammatory cell accumulation.
Bianchi M (2019)	34	68% in persistent/chronic CSCR	HRF presence and coarse morphology suggest degenerative or phagocytic activity.
de Carlo TE (2015)	50	80% in eyes with SRF > 3m months	HRF may represent lipofuscin or macrophages, linked with chronic leakage.
Matet A (2019)	72	65.4% overall	Strong link between HRF granularity and chronicity markers like PED or thinning.

Table 4. Studies Supporting OCT/OCT-A role in detection of CNV in CSCR

Study	Sample Size (Eyes)	Prevalence	Key Findings
Huang (2014)	102	43%	OCT-A identified CNV in 43% vs 21% with FA; improved detection of non-leaking CNV.
Bonini (2015)	27	30%	OCT-A detected 100% of CNV lesions featured in FFA
Costanzo (2015)	66	33%	OCT-A outperformed FA/ICGA in detecting subclinical CNV; earlier treatment potential.
Mousa (2017)	60	8%	Foveal thinning, irregular flat PED, and increased choroidal thickness are risk factors for CNV development.
Spaide (2018)	89	38%	Branching CNV networks detected in cases misclassified by FFA.
Haggag (2022)	163	33%	Hyperreflective space beneath PED indicates a higher risk of CNV detection than Double layer sign in OCT

Figures

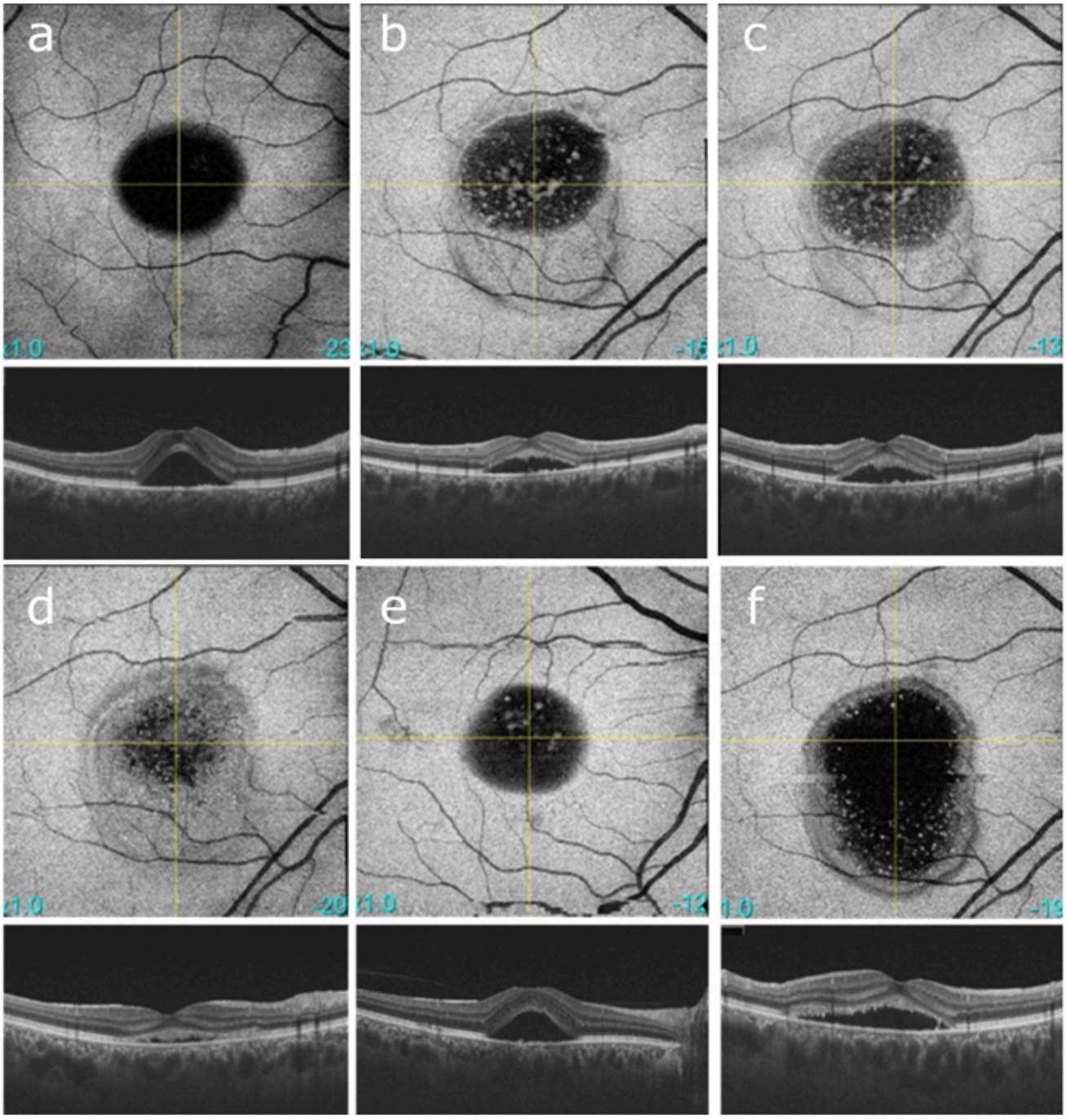


Figure 1

High Reflective Foci (HRF) morphology in various subtypes of CSCR. In Acute CSCR, HRF were not detected in any patient (a). On the other hand, mixture of fine dispersed & coarse HRF were found in persistent CSCR (b, c). In chronic CSCR, only fine pattern HRF were detected (d-f).

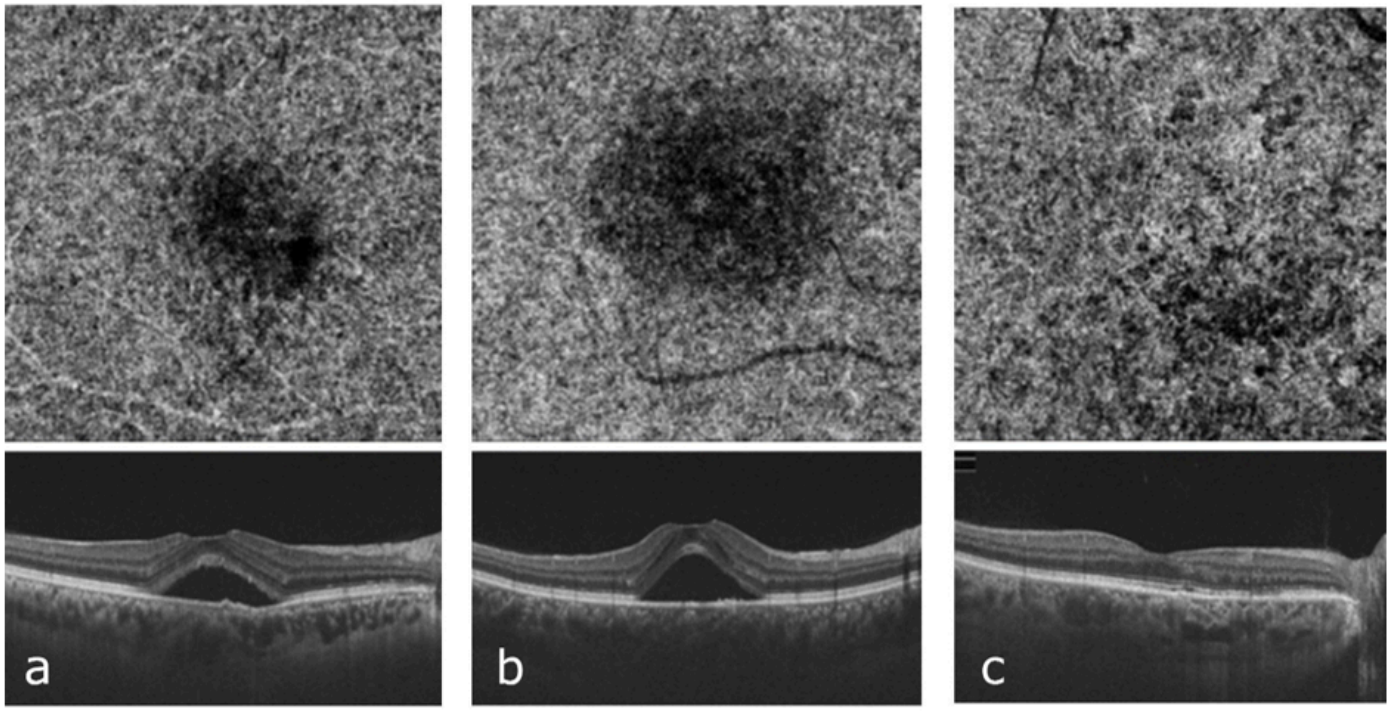


Figure 2

Distribution of Choriocapillaris (CC) hypoperfusion in different CSCR subtypes. In acute and persistent CSCR, patchy areas of CC hypoperfusion were confined to areas of subretinal fluid (a, b). On the contrary, patchy CC hypoperfusion extended diffusely in the choroid (c).

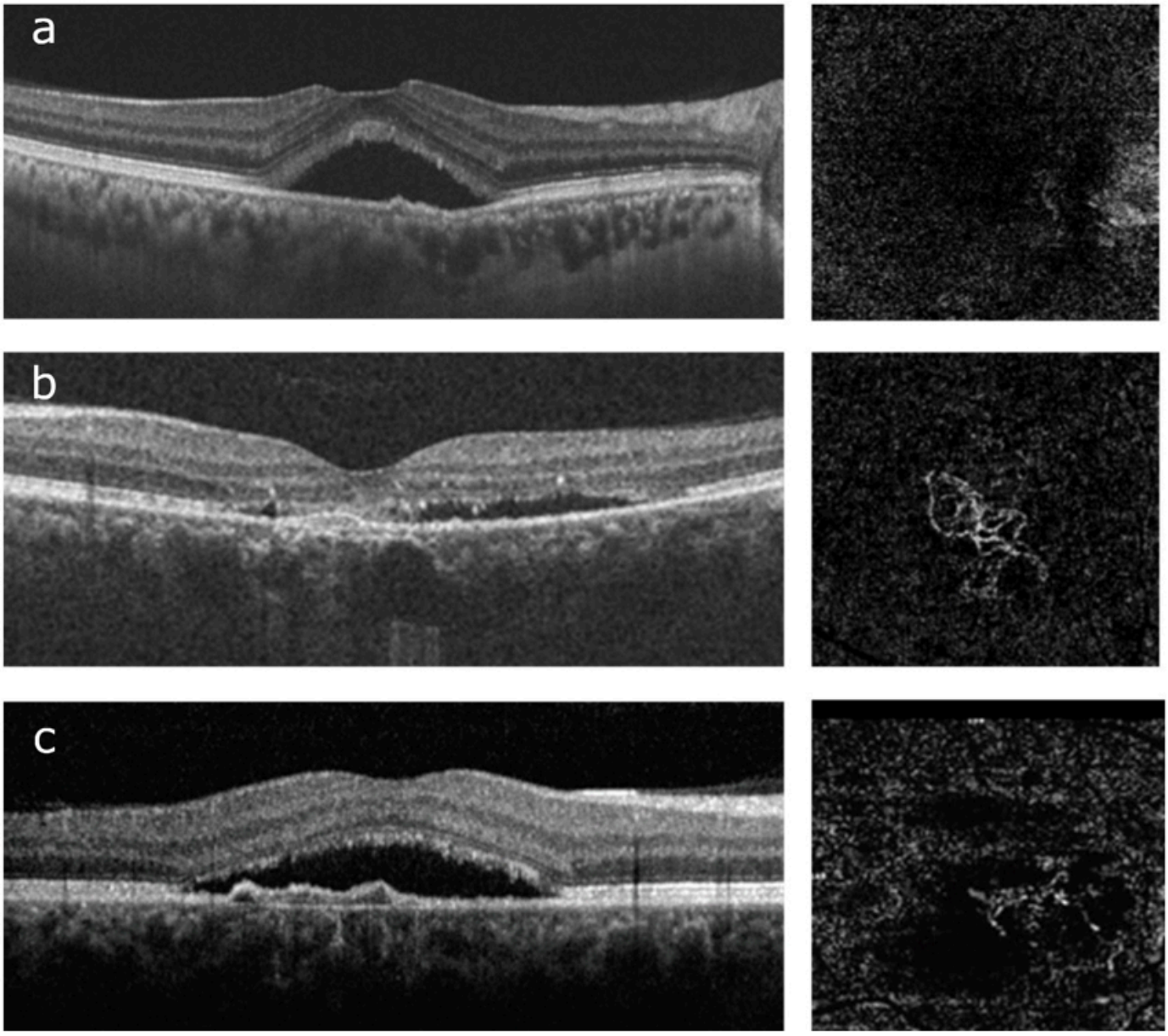


Figure 3

OCT Angiography characterization of CVN morphology in CSCR. Three patterns were identified in OCT-A slabs under FI-PED, poorly-defined pattern (a), branching pattern (b), and immature pattern (c).